PCCP

ROYAL SOCIETY OF CHEMISTRY

PAPER

View Article Online
View Journal | View Issue

Cite this: *Phys. Chem. Chem. Phys.*, 2025, **27**, 7826

Influence of substitution patterns on isomer preference in 1 : 1 chromone–methanol complexes†

Natalia Moreira Cárcamo, [a] Patrick H. Strebert[b] and Fabian Dietrich *[a]

Received 27th January 2025,
Accepted 24th March 2025

DOI: 10.1039/d5cp00374a

rsc.li/pccp

The cluster formed by chromone and methanol serves as an excellent model for studying the various contributions to intermolecular interaction energy. The asymmetric ketone motif of chromone provides distinct hydrogen-bonding sites, enabling differentiation between an ''inside'' and an ''outside'' isomer using infrared spectroscopy. We employ DFT simulations to assess how functional groups influence the balance between the two isomers and to identify derivatives that switch their isomer preference upon electronic excitation. We identify three mono-substituted and four doubly substituted chromone derivatives that meet these criteria. Additionally, the contributions to intermolecular interactions are examined using the local energy decomposition method.

1. Introduction

The importance of a good interplay between experimental and theoretical chemistry is well recognized nowadays. As both benefit from close coexistence,[1] several challenges have been created by the experimentalists to encourage the theoretical community to provide the best results for *e.g.* structural preferences of furan derivatives with methanol[2,3] or prediction of the vibrational frequencies of water clusters of a list of hydrogen bond acceptors.[4]

The experimental study of selected molecular systems can serve as valuable benchmarks for theoretical chemistry, enabling the testing of newly developed methods. These molecular systems are particularly useful when they represent a near-equilibrium state between at least two distinct states. During the last decade, several systems have been investigated with respect to the influence of London dispersion interactions. Infrared and microwave spectroscopy were applied under molecular beam conditions to differentiate OH–O and OH–π binding motifs of various alcohols with diphenyl ether,[5–9] phenyl vinyl ether,[10] and dibenzofuran.[11] A similar question regarding the preferred binding sites of hydrogen bonds has been explored for asymmetric ketones.[12,13] In this context, we examined the chromone–methanol aggregate using mass-selective IR/UV spectroscopy in a molecular beam.[14] The competition in this system arises from the binding site of methanol. Due to the structure of chromone, two distinct pockets are formed: an inner and an outer pocket. For pristine chromone in the electronic ground state (S_0), the outer pocket is preferred by a value of 1.2 kJ mol^{-1} over the inner pocket. This preference is augmented in the first excited triplet state (T_1), yielding an energy difference of 4.0 kJ mol^{-1}. This preference was confirmed by the investigation of the corresponding O–H stretching frequency.

For the above mentioned benchmarking process, it would be of great interest to study an aggregate, whose binding site preference changes upon electronic excitation. With the investigation of such an aggregate, the dynamics of the pocket preference of methanol can be studied, which gives an additional challenge for the theoretical methods. To expand the scope of the chromone–methanol system,[14] two possible routes can be taken to to probe non-covalent interactions in the electronic ground and excited triplet state. Firstly, the coordinating solvent molecule can be changed from methanol to water or *tert*-butanol similar to prior investigations on aromatic ether-solvent complexes.[5–8,10,11] However, another possibility to influence the carbonyl balance is an adequate derivatization of the chromone molecule. This is comparable to investigations on substituted acetophenone-solvent complexes by the Suhm group.[12,13] These two approaches can be certainly combined, but here we want to focus our investigation on clusters formed by chromone derivatives and methanol.

In this study, we employ DFT simulations to investigate chromone derivatives, focusing on how functional groups influence the balance between the inside and outside binding sites of the methanol molecule in both the S_0 (ground) and T_1 (triplet excited) states. Our first objective is to determine whether the energy difference (ΔE) between the two binding sites can be systematically adjusted in both states. Ultimately, the goal is to either shift the overall binding preference from the

[a] *Departamento de Ciencias Físicas, Universidad de La Frontera, Francisco Salazar, 01145, Temuco, Chile. E-mail: fabian.dietrich@ufrontera.cl*
[b] *Chemistry Department, RPTU Kaiserslautern, Kaiserslautern, Germany*

† Electronic supplementary information (ESI) available. See DOI: https://doi.org/10.1039/d5cp00374a

outside to the inside pocket or achieve an equilibrium between the two motifs. This allows potent benchmarking studies probing the binding preference experimentally and subsequent comparison with quantum-chemical calculations similar to already published benchmarking efforts.[2–4,15,16] Therefore, the accuracy of quantum-chemical methods, especially with regard to hydrogen-bonded clusters, can be improved and the role of dispersion in excited states elucidated. The analysis of intermolecular interactions in excited states is challenging and only a few methods have been developed in the last years. Here, we would like to mention energy decomposition approaches based on absolutely localized molecular orbitals,[17,18] time-dependent DFT,[19,20] multi-state DFT[21–23] or multi configurational symmetry adapted perturbation theory, SAPT(MC),[24,25] the last one recently applied to a similar system, anisole-water.[26] For our investigations here, we apply the local energy decomposition (LED[27]) method base on single point DLPNO-CCSD(T) simulations, analyzing the contribution of dispersion, non-dispersion, electrostatics and exchange in the electronic ground state and first excited triplet state.

2. Theoretical methods

Ground state properties of all discussed chromone derivatives with methanol were simulated using density functional theory (DFT) with the CAM-B3LYP[28–30] functional, a def2-TZVPP[31] basis set and D3 dispersion correction including Becke–Johnson damping.[32] This combination was already been used in our former study[14] and yielded a good agreement with the experimental data. Geometry optimizations were performed and the identity of a minimum structure was checked with calculating the Hessian, finding no negative eigenvalues. For the SCF convergence the !TightSCF keyword of ORCA was used, corresponding to a convergence criterion of 1.0×10^{-9} E_h. The geometry convergence was reached with the tightopt keyword, corresponding to a tolerated energy change of 1.0×10^{-6} E_h. We used ORCAs default DFT grid (!defgrid2). The T_1 was treated as ground state, using unrestricted open–shell DFT. Theoretical harmonic wavenumbers of the molecular vibrations are obtained from an analytical frequency calculation and reported without applying a scaling factor.

We analyzed the optimized structures with respect to the contributions of different intermolecular interactions applying the local energy decomposition (LED) method[27,33–36] on basis of DLPNO-CCSD(T)[37,38] single point calculations, applying the resolution of identity (RIJK). As basis set def2-TZVP[31,39] was chosen, furthermore the "TightPNO" option was selected. All simulations were performed with ORCA 6.0.0.[40,41] Visualizations of structures were made with Avogadro 1.20.[42] For the visualization of the dispersion interaction densities (DID),[43] we obtained the densities with the orca_plot package in a $80 \times 80 \times 80$ grid. The DIDs were mapped on the electron density using UCSF ChimeraX.[44]

3. Results and discussion

The first step is to identify suitable chromone derivatives. This involves modulating the electronic properties of the chromone molecule to selectively shift the energy balance in favor of the inside isomer over the outside one. However, since both motifs involve the carbonyl bond, distinguishing between the two lone pairs on the carbonyl oxygen is challenging. One potential approach is to introduce electron-withdrawing groups (*e.g.*, F, CF_3, NO_2), which could weaken the hydrogen bond. This weakening might stabilize the inside motif, as the outside motif relies on a stronger hydrogen bond that contributes more significantly to the binding energy. Nevertheless, the introduction of such groups may also reduce the polarizability of the system through negative inductive and/or mesomeric effects, thereby diminishing the influence of dispersion forces.

The chromone molecule features six aromatic C–H bonds, all of which are potential sites for substitution (see Fig. 1). However, the hydrogen atoms at positions 3 and 5 are essential for forming a C–H···O interaction with the methanol molecule. Introducing a dispersion energy donor at position 6 could stabilize the inside motif due to its close proximity to the relevant C–H bond. Similarly, functional groups at position 2 might further stabilize the outside isomer. In contrast, substituents at positions 7 and 8 are expected to have only a minimal effect on the balance between the two binding sites. Consequently, our analysis focuses on chromone derivatives with functional groups at positions 2 and 6.

For the investigation in both electronic states, we chose the following list of substituents: $-CF_3$, –CHO, –Cl, –CN, –COOH, –Et, –F, –Me, –NC, –NCO, $-NH_2$, $-NO_2$, –OCN, –OH, –OMe, –Ph, $-SiH_3$, $-SiMe_3$, $-SO_3H$, and –*t*Bu. These functional groups include both electron-withdrawing and electron-donating substituents, as well as bulky groups that act as dispersion energy donors. For the forthcoming analysis, we will only consider the competition between inside and outside isomers. A competition of a structural motif, where the methanol binds to the ether oxygen can be excluded, since the energy difference is about 18 kJ mol^{-1} (ref. 14) for chromone and in a similar range for the derivatives, see ESI,† Table S10. In a similar matter, we can exclude the structural motifs of methanol binding to functional groups like –CHO, –COOH, $-NO_2$, and $-SO_3H$, having higher relative energies.

3.1. Ground state properties of mono substituted chromone

For both substitution positions, the 20 functional groups are introduced for the inside and the outside isomer, exemplarily shown for 2-methyl chromone in Fig. 2.

As reported for the pristine chromone, the energy difference $\Delta E = E_{\text{inside}} - E_{\text{outside}}$ between the two isomers is small

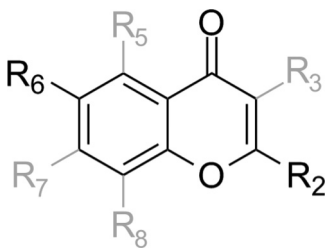

Fig. 1 Substitution positions in chromone.

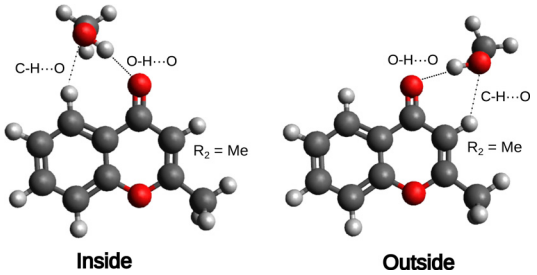

Fig. 2 Differentiation of the isomers "inside" and "outside" with respect to the binding side relative to the carbonyl group.

(1.2 kJ mol^{-1} (ref. 14)). Hence, we also analyze the values obtained for the substituted chromone derivatives. The results can be found in Table S1 in the ESI.† The values of ΔE (including zero-point corrections) show a range between −0.23 kJ mol^{-1} (–NO_2) and +4.71 kJ mol^{-1} (–SO_3H) for substitution position 2, and between −3.79 kJ mol^{-1} (–$SiMe_3$) and +5.81 kJ mol^{-1} (–SO_3H) for substitution position 6.

The experimental differentiation of the isomers depends on the observable wavenumber of the O–H vibration, modulated by the strength of the hydrogen bond between methanol and the carbonyl group of chromone. Hence, Table S1 (ESI†) also contains the calculated (unscaled) wavenumber of the O–H stretching vibration. We want to notice here that for some derivatives, experimental problems may occur due to the overlap of bands in the interval between 3400 and 3700 cm^{-1}. This can be expected for functional groups with additional O–H and N–H moieties like –COOH, –NH_2, –OH and –SO_3H. In Fig. 3, the difference of the wavenumbers of the O–H stretching vibration ($\Delta\tilde{\nu} = \tilde{\nu}_{\text{inside}} - \tilde{\nu}_{\text{outside}}$) are plotted against the energy difference of the isomers. Fig. S1 (ESI†) (first line) shows the wavenumber of the outside isomer against the inside isomer. Both substitution positions exhibit a direct proportionality of the wavenumbers, meaning that the strength of the red-shift in the O–H vibration of methanol induced by functional groups will be affected similarly in both pockets. Regarding the correlation between the energy shift and the wavenumber difference, a direct correlation is observed only for substituents at position 2. For position 6, the data points are more scattered, which results in a lower R^2 value for the linear fit. This suggests that substituents at position 2 have a more significant impact on the O–H···O interaction, while substituents at position 6 appear to exert a more indirect influence, such as enhancing the dispersion interaction.

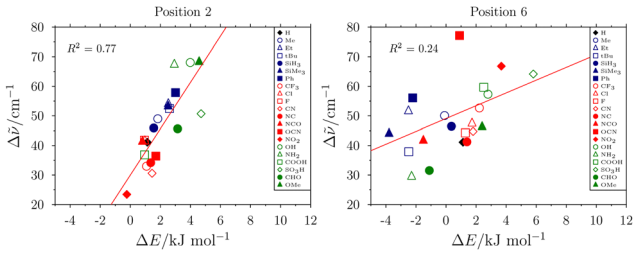

Fig. 3 Results of energy differences between ΔE and O–H vibration shifts $\Delta\tilde{\nu}$ between inside and outside in the S_0 state.

3.2. Excited state properties of mono substituted chromone

For the investigation of the first excited triplet state, different methodologies exist including unrestricted DFT, time-dependent DFT, configuration interactions or coupled cluster variants like SCS-CC2. For the later reported energy decomposition methods, it is necessary to treat the triplet as a ground state, hence we used here the unrestricted DFT method, changing the multiplicity for these calculations.

The simulation of the triplet state turns out to be more challenging than the corresponding singulet. As the chromone molecule is aromatic in the S_0 state, an identical structure in the T_1 state should be an antiaromat following Baird's rule.[45–47] In order to avoid the antiaromaticity, a distortion of at least one ring is expected. This distortion behavior was reported for the pyrone ring, *e.g.*, in γ-pyrone[48] and psoralene[49] as well as in our former investigation of the pristine chromone.[14]

We initially expected that the distortion of the pyrone ring (referred to as "puckering") would represent the minimum on the potential energy surface of the chromone backbone. Therefore, we began the optimizations of the substituted chromones from the corresponding planar structures of the S_0 state. However, this approach was not successful for all derivatives. As a result, we restarted the search, this time beginning with a puckered conformer. Specifically, we used the chromone backbone structure obtained from the puckered 2-Cl derivative as the starting point. In sum, three different optimization behaviors were detected: (1) planar ⇒ puckered; (2) planar ⇒ planar, puckered ⇒ puckered; (3) puckered ⇒ planar. Fig. 4 shows a scheme of these cases.

Case 1 represents the expectation. The planar conformer is not a minimum in the T_1 state and the optimization runs into a puckered conformer. Case 1 is observed in 42 of 80 simulations, with a higher percentage for substituents in position 6. Case 2 represents the coexistence of (at least) two triplet states with different dihedral but with similar energy. Due to an energy barrier between planar and puckered structure, the dihedral will not change significantly during optimization process and both conformers can be found as (local) minima. In Fig. 4, we differentiate between two sub-cases: (a) the puckered conformer is more stable than the planar one, and (b) the planar conformer is the global minimum. Case 2a is observed in 9 and case 2b in 10 of the overall 80 simulations. Case 3 represents the exclusive existence of the planar conformer, making it impossible to obtain a puckered one. This case is observed for 19 of 80 simulations. The differentiation between planar and puckered conformers is shown in Tables S2 and S3 (ESI†). We would like to highlight a few special cases. For the 2-Et, 2-F, and 2-NC derivatives, a stable puckered conformer is only found for the inside isomer. In these three cases, the energy difference between the puckered and planar conformers is about 300 kJ mol^{-1}, which corresponds to case 2b. These large energy differences suggest that the potential energy curve is close to case 3. Therefore, even a small perturbation, such as a change in the position of the methanol molecule, could cause the barrier to disappear, resulting in the loss of a local minimum for the puckered conformer.

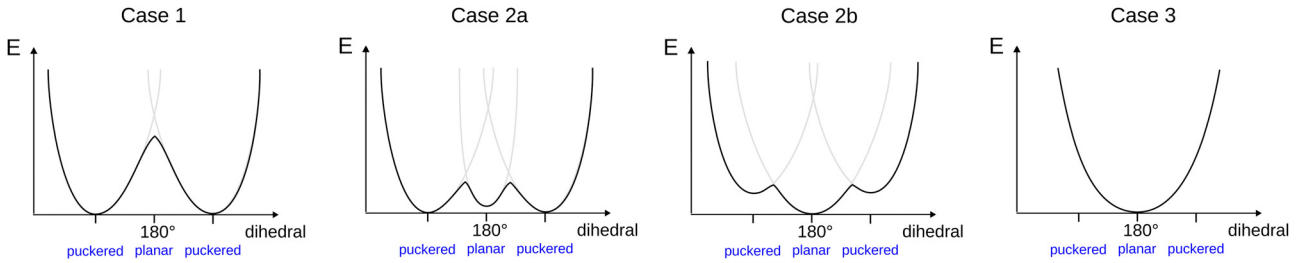

Fig. 4 Schematic description of the observed behaviors of several chromone derivatives during the optimization in the T_1 state.

We are aware that this behavior might be specific for the used UDFT method (and probably related to the used functional), since more expensive methods like configuration-interaction or coupled-cluster might find the puckered structure for all derivatives as already discussed for the pristine chromone.[14] However, these methods do not yield suitable frequency simulations, which are necessary for comparison with experimental data.

In the majority of the derivatives, the puckered structure is the minimum structure as it is in the case of the pristine chromone. Hence, we decided to compare the energies and wavenumbers in Fig. 5 and Fig. S1 (ESI†) (second line) for the puckered conformers only. The corresponding energies when the optimizations yield also planar isomers are shown in Tables S2 and S3 (ESI†). In the cases of not finding stable puckered conformers, the corresponding derivatives are omitted for the analysis in Fig. 5.

Similar to the electronic ground state, a proportionality of the wavenumbers of the inside isomer and the outside isomer can be found, indicating that the strength of the hydrogen bond is also modulated by the pocket in triplet state. Furthermore, there is a slight tendency that a larger energy gap between inside and outside isomer is correlated with a higher splitting of the wavenumbers of the O–H stretching frequencies. However, we can use only 10 values for position 2 and for position 6, the scattering of the values is high with an R^2 values of 0.29.

The objective of our investigation is to identify chromone derivatives where the preference for the inside or outside isomer switches upon electronic excitation. From the pristine chromone, it is known that the energy preference for the outside isomer increases from 1.2 kJ mol^{-1} in the S_0 to 4.0 kJ mol^{-1} in the T_1 state. Using these reference data, we hypothesize that the switching is only possible for the direction S_0(inside) → T_1(outside) but not S_0(outside) → T_1(inside). Therefore, we need to look for derivatives with a $\Delta E(S_0)$ below 0 kJ mol^{-1} and a $\Delta E(T_1)$ above 0 kJ mol^{-1}. Fig. 6 illustrates the correlation between the energy differences in the S_0 and T_1 state, depending on the substitution position. The gray areas represent the energy ranges of 2 kJ mol^{-1} for both electronic states, since we expect the $\Delta\Delta E$ to be between 0 and 4 kJ mol^{-1}. Those derivatives, which show the switch of the preferred binding site, should be within the dark gray area. All derivatives with the substituent in position 2 are outside this area, which means none of them shows the desired change from inside to outside upon electronic excitation. For all derivatives, the outside isomer is preferred independent of the electronic state‡. In contrast, for derivatives in with substituents in position 6, we found also preference for the inside isomer both in the S_0 and T_1 state. In fact, a good correlation between $\Delta E(S_0)$ and $\Delta E(T_1)$ can be found. The slope of the red line is 1.1 with an intercept of 2.2 kJ mol^{-1}, confirming that the switching can only be S_0(inside) → T_1(outside). Within the dark gray area, three derivatives are found: 6-CHO, 6-Me, and 6-NCO. These are promising candidates for an experimental investigation. Their corresponding vibrational frequencies are separated by at least 30 cm^{-1} which should provide the possibility to distinguish the isomers in the experiment.

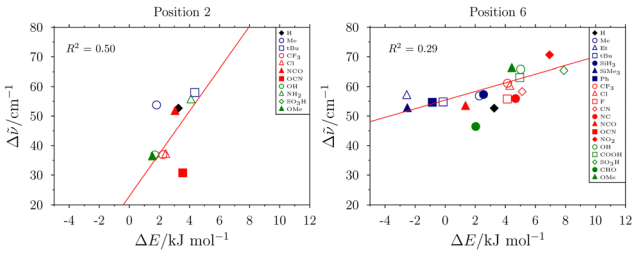

Fig. 5 Results of energy differences between ΔE and O–H vibration shifts $\Delta\tilde{\nu}$ between inside and outside in the T_1 state.

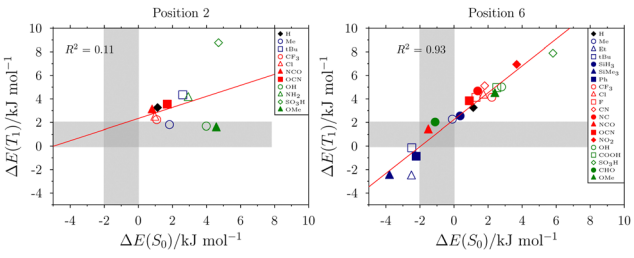

Fig. 6 Results of energy differences ΔE between inside and outside for the S_0 and T_1 states.

3.3. Doubly substituted chromone

As shown in Fig. 6, certain derivatives with electron-donating groups such as $SiMe_3$, Et or *t*Bu in position 6 exhibit negative ΔE values in both the S_0 and the T_1 states. In contrast, all substituents in position 2 result in positive ΔE values. This raises the question of whether the substitution effects are

‡ The only derivative with $\Delta E(S_0) < 0$, 2-NO_2, does not yield a puckered conformer in the T_1 state.

additive and if combining substitutions could yield ΔE values within the desired range. To explore this, we investigated an additional set of fifteen derivatives, combining 2-CF_3, 2-Cl, and 2-NCO with 6-CHO, 6-Me, 6-NCO, 6-OCN and 6-*t*Bu. The results with respect to energies and vibrational frequencies are shown in Tables S4 and S5 (ESI†).

Fig. 7 shows the differences of the vibrational frequencies and the energy differences of the inside and outside isomer. In the S_0 state, a cumulation of derivatives with the same functional group in position 6 can be found, indicated by the color. This means, that the influence of the substituent in position 6 is larger than the substituent in position 2. This finding is in accordance with the results shown in Fig. 3, showing a larger energy range for the 6-derivatives than the 2-derivatives. Within a group of double substituted chromone derivatives with the same group in position 6, a pattern can be found, indicating that the 2-CF_3 derivative shows the lowest wavenumber and the highest energy difference, while the 2-NCO derivative has the lowest energy difference between inside and outside isomer. Similar patterns can be found in the T_1 state. However, here the values are more distributed over the whole energy interval. In all cases, the 2-NCO derivative has the largest wavenumber and highest energy difference, while the 2-CF_3 derivatives yield the smallest wavenumber and smallest energy difference.

With respect to the switching preference from the inside isomer in the S_0 state to the outside isomer in the T_1, we analyze again the intervals of 2 kJ mol^{-1} around the equilibrium. This analysis is shown in Fig. 7 right. Within the gray area (or very close to the border), four derivatives are found. It is the trio of derivatives having the 6-Me group in common and differ only slightly by their substituent in position 2. Furthermore, the doubly NCO substituted chromone also shows the preference switching. Evaluating the wavenumber difference of the four derivatives, we can state that the corresponding value in the S_0 state ranges between 30 and 40 cm^{-1} and in the T_1 state between 30 and 50 cm^{-1}. Hence, these four derivatives are also good candidates for the experimental investigation.

3.4. Analyses of intermolecular interactions

As already discussed for the pristine chromone–methanol cluster, the preference of the binding motif depends on the delicate interplay between different contributions of the intermolecular interaction.[14] In order to illuminate this interplay and to also study the difference of those contributions in dependence on the electronic state, we applied the methodology of local energy decomposition giving an overview of the contributions of electrostatics ($E^{\text{ref.}}_{\text{elstat}}$), exchange ($E^{\text{ref.}}_{\text{exch}}$), electronic deformation ($\Delta E^{\text{ref.}}_{\text{el-prep}}$), dispersion ($E^{\text{C-CCSD}}_{\text{dispersion}}$) and non-dispersion ($\Delta E^{\text{C-CCSD}}_{\text{non-dispersion}}$) to the intermolecular interaction energy. In Tables S6–S9 (ESI†), all contributions of the LED analysis are given, differentiating the inside and outside isomer, both in the S_0 and T_1 state. We limited our analyses to those derivatives, which we have been found to be of interest due to their predicted switching preference.

For all investigated systems, we can state that the overall interaction energies are quite similar. In the S_0 state, values are found in the range of −33 and −35 kJ mol^{-1}. In the T_1 state, those interactions energies are smaller, ranging from −29 to −31 kJ mol^{-1}, with the exception of (2-NCO, 6-NCO)-chromone. Comparing those values to the pristine chromone–methanol cluster,[14] a small decrease of the interaction energy is found. This indicates that the substituents enhance the stability of the cluster. Furthermore, it can be seen that the inside conformer contains a more significant contribution of dispersion interaction than the corresponding outside isomer. The origin can be seen analyzing the DID plots. In Fig. 8, the difference between inside and outside is exemplarily shown. The DID plots for all analyzed clusters can be found in Fig. S2 (ESI†).

It can be seen that the difference of the isomers is the C–H···O interaction from the aromatic C–H bond to the methanol. In the case of the inside isomer, the orange part signalizes a stronger contribution than the corresponding green C–H in the outside isomer. Furthermore, the methyl group of the methanol molecule in the inside isomer is green in comparison the blue group in the outside isomer, indicating a higher contribution of dispersion interaction also in the methanol molecule. Considering the energy differences of dispersion energy between the isomers, values of 2–4 kJ mol^{-1} are observed for the 6-substituted chromone derivatives. Interestingly, this difference decreases for the doubly substituted derivatives. Comparing the electronic states, no significant difference for the contribution of dispersion can be found. Depending on the particular derivative, large distributions to the intermolecular interaction energy can be found for the electrostatic

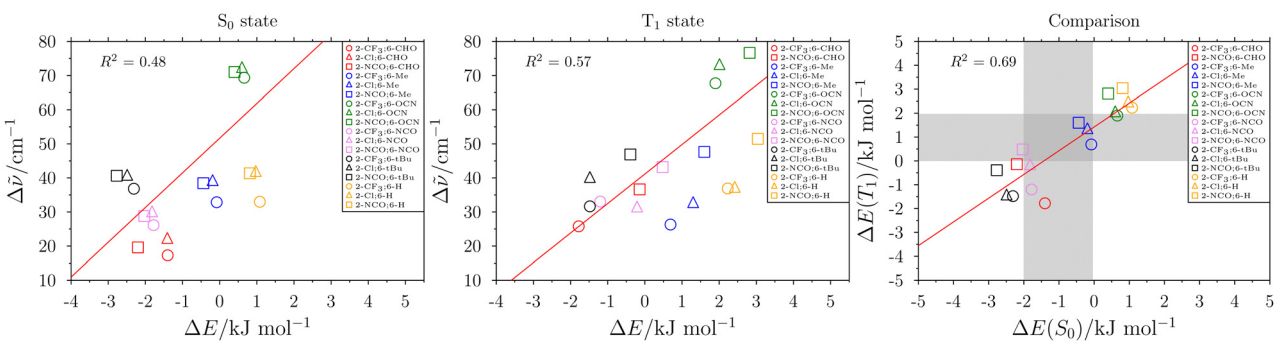

Fig. 7 Results of energy differences between ΔE and O–H vibration shifts $\Delta\tilde{\nu}$ between inside and outside for S_0 and T_1 four doubly substituted chromone derivatives. In yellow, three mono substituted derivatives are shown for comparison.

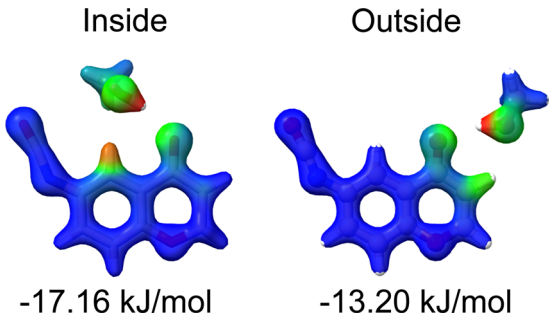

Fig. 8 Dispersion interaction density plot for 6-NCO in the T_1 state. Red and blue color represent a large and small contribution of the dispersion interaction, respectively. Energy values are given for $E^{C\text{-}CCSD}_{dispersion}$.

energy as well as the electronic preparation energy. Although here larger differences between the two isomers can occur, these two contributions normally compensate each other, which yield consistent results with respect to the difference of the interaction energy. In order to demonstrate this, we compared this difference with the difference of the DLPNO-CCSD(T) energies in the Tables S6–S9 (ESI†). These values are almost equal. Both the DLPNO-CCSD(T) energy and the sum of the intermolecular interactions applying the LED analyses show the preference of the inside isomer in the S_0 and the preference of the outside isomer in the T_1 state. With these results, we can confirm the performance of the used dispersion corrected DFT method in the evaluation of the preference switching. Only the 2-NCO, 6-NCO chromone, which shows an unusual increase of interaction energy in the T_1 state, does not coincide with the prediction of the DFT simulations. Relying on the DLPNO-CCSD(T) method, the inside isomer is energetically favored in both electronic states. Hence, an experimental investigation would be even more of interest to evaluate the performance of DLPNO-CCSD(T) and DFT in this particular case.

4. Conclusion

We performed dispersion-corrected DFT simulations to find chromone derivatives, whose methanol complexes change their preferred binding site by excitation from the electronic ground state to the first excited triplet state. This work should be used to initiate the experimental investigation of those clusters. Experimental evidence of the preference switch (or not switch) can be thought as benchmarks for the validation of more sophisticated theoretical methods, considering also the importance of dispersion interactions in excited electronic states. The screening of the chromone derivatives revealed seven candidates, which show a preference of the inside isomer in the S_0 state and a preference of the outside isomer in the T_1 state. These derivatives are the three mono-substituted compounds 6-CHO-chromone, 6-Me-chromone and 6-NCO-chromone and the four double substituted compounds (2-CF_3, 6-Me)-chromone, (2-Cl, 6-Me)-chromone, (2-NCO, 6-Me)-chromone and (2-NCO, 6-NCO)-chromone. The energy decomposition analyses show that the inside isomers show larger contributions of dispersion interaction than the outside isomers due the strong interaction between the aromatic C–H and the O of methanol. However, this contribution is compensated by other contributions like the non-dispersion, electrostatics and electronic preparation. Hence, the balance between the contributions is quite delicate and the preferences are not easy to predict. On the other hand, this implies these clusters are very good candidates for an experimental–theoretical challenge in the future.[50,51]

Author contributions

Conceptualization: P. S., F. D.; methodology: P. S., F. D.; software: P. S., F. D., validation: F. D.; formal analysis: N. M., F. D., investigation: N. M., P. S., F. D.; resources: F. D., data curation: N. M., F. D.; writing – original draft: N. M., P. S., F. D., writing – review & editing: F. D., visualization: N. M., F. D., supervision: F. D.; project administration: F. D.; funding acquisition: F. D.

Data availability

Data for this article, including input structures and ORCA outputs are available at ZENODO repository at **https://doi.org/10.5281/zenodo.14750557**.

Conflicts of interest

All authors declare that they have no conflicts of interest.

Acknowledgements

F. D. thanks the Agencia Nacional de Investigación y Desarollo (ANID) for financial support of this research in project FONDECYT de Iniciación 11230223. N. M. and F. D. acknowledge partial financial support from the project "Implementación de una unidad interdisciplinar para el desarrollo de Tecnologías Aplicadas y Ciencias (InTec)", Code "FRO2395", from the Ministry of Education of Chile. Powered@NLHPC: This research was partially supported by the supercomputing infrastructure of the NLHPC (CCSS210001).

Notes and references

1 R. A. Mata and M. A. Suhm, *Angew. Chem., Int. Ed.*, 2017, **56**, 11011–11018.
2 H. C. Gottschalk, A. Poblotzki, M. A. Suhm, M. M. Al-Mogren, J. Antony, A. A. Auer, L. Baptista, D. M. Benoit, G. Bistoni, F. Bohle, R. Dahmani, D. Firaha, S. Grimme, A. Hansen, M. E. Harding, M. Hochlaf, C. Holzer, G. Jansen, W. Klopper, W. A. Kopp, L. C. Kröger, K. Leonhard, H. Mouhib, F. Neese, M. N. Pereira, I. S. Ulusoy, A. Wuttke and R. A. Mata, *J. Chem. Phys.*, 2018, **148**, 014301.
3 H. C. Gottschalk, A. Poblotzki, M. Fatima, D. A. Obenchain, C. Pérez, J. Antony, A. A. Auer, L. Baptista, D. M. Benoit, G. Bistoni, F. Bohle, R. Dahmani, D. Firaha, S. Grimme, A. Hansen, M. E. Harding, M. Hochlaf, C. Holzer, G. Jansen,

W. Klopper, W. A. Kopp, M. Krasowska, L. C. Kröger, K. Leonhard, M. Mogren Al-Mogren, H. Mouhib, F. Neese, M. N. Pereira, M. Prakash, I. S. Ulusoy, R. A. Mata, M. A. Suhm and M. Schnell, *J. Chem. Phys.*, 2020, **152**, 164303.

4 T. L. Fischer, M. Bödecker, S. M. Schweer, J. Dupont, V. Lepère, A. Zehnacker-Rentien, M. A. Suhm, B. Schröder, T. Henkes, D. M. Andrada, R. M. Balabin, H. K. Singh, H. P. Bhattacharyya, M. Sarma, S. Käser, K. Töpfer, L. I. Vazquez-Salazar, E. D. Boittier, M. Meuwly, G. Mandelli, C. Lanzi, R. Conte, M. Ceotto, F. Dietrich, V. Cisternas, R. Gnanasekaran, M. Hippler, M. Jarraya, M. Hochlaf, N. Viswanathan, T. Nevolianis, G. Rath, W. A. Kopp, K. Leonhard and R. A. Mata, *Phys. Chem. Chem. Phys.*, 2023, **25**, 22089–22102.

5 C. Medcraft, S. Zinn, M. Schnell, A. Poblotzki, J. Altnöder, M. Heger, M. A. Suhm, D. Bernhard, A. Stamm, F. Dietrich and M. Gerhards, *Phys. Chem. Chem. Phys.*, 2016, **18**, 25975–25983.

6 D. Bernhard, F. Dietrich, M. Fatima, C. Perez, A. Poblotzki, G. Jansen, M. A. Suhm, M. Schnell and M. Gerhards, *Phys. Chem. Chem. Phys.*, 2017, **19**, 18076–18088.

7 D. Bernhard, C. Holzer, F. Dietrich, A. Stamm, W. Klopper and M. Gerhards, *ChemPhysChem*, 2017, **18**, 3634–3641.

8 F. Dietrich, D. Bernhard, M. Fatima, C. Pérez, M. Schnell and M. Gerhards, *Angew. Chem., Int. Ed.*, 2018, **57**, 9534–9537.

9 M. Fatima, D. Maué, C. Pérez, D. S. Tikhonov, D. Bernhard, A. Stamm, C. Medcraft, M. Gerhards and M. Schnell, *Phys. Chem. Chem. Phys.*, 2020, **22**, 27966–27978.

10 D. Bernhard, F. Dietrich, M. Fatima, C. Pérez, H. C. Gottschalk, A. Wuttke, R. A. Mata, M. A. Suhm, M. Schnell and M. Gerhards, *Beilstein J. Org. Chem.*, 2018, **14**, 1642–1654.

11 D. Bernhard, M. Fatima, A. Poblotzki, A. L. Steber, C. Pérez, M. A. Suhm, M. Schnell and M. Gerhards, *Phys. Chem. Chem. Phys.*, 2019, **21**, 16032–16046.

12 C. Zimmermann, H. C. Gottschalk and M. A. Suhm, *Phys. Chem. Chem. Phys.*, 2020, **22**, 2870–2877.

13 C. Zimmermann, M. Lange and M. A. Suhm, *Molecules*, 2021, **26**, 4883.

14 P. Boden, P. H. Strebert, M. Meta, F. Dietrich, C. Riehn and M. Gerhards, *Phys. Chem. Chem. Phys.*, 2022, **24**, 15208–15216.

15 A. Poblotzki, H. C. Gottschalk and M. A. Suhm, *J. Phys. Chem. Lett.*, 2017, **8**, 5656–5665.

16 T. L. Fischer, M. Bödecker, A. Zehnacker-Rentien, R. A. Mata and M. A. Suhm, *Phys. Chem. Chem. Phys.*, 2022, **24**, 11442–11454.

17 Q. Ge and M. Head-Gordon, *J. Chem. Theo. Comput.*, 2018, **14**, 5156–5168.

18 Q. Ge, Y. Mao and M. Head-Gordon, *J. Chem. Phys.*, 2018, **148**, 064105.

19 P. Su, Z. Jiang, Z. Chen and W. Wu, *J. Phys. Chem. A*, 2014, **118**, 2531–2542.

20 Z. Tang, B. Shao, W. Wu and P. Su, *Phys. Chem. Chem. Phys.*, 2023, **25**, 18139–18148.

21 Y. Lu and J. Gao, *J. Phys. Chem. Lett.*, 2022, **13**, 7762–7769.

22 R. Zhao, C. Hettich, J. Zhang, M. Liu and J. Gao, *J. Phys. Chem. Lett.*, 2023, **14**, 2917–2926.

23 C. P. Hettich, X. Zhang, D. Kemper, R. Zhao, S. Zhou, Y. Lu, J. Gao, J. Zhang and M. Liu, *J. Am. Chem. Soc. Au*, 2023, **3**, 1800–1819.

24 M. Hapka, A. Krzemińska, M. Modrzejewski, M. Przybytek and K. Pernal, *J. Phys. Chem. Lett.*, 2023, **14**, 6895–6903.

25 M. R. Jangrouei, A. Krzemińska, M. Hapka, E. Pastorczak and K. Pernal, *J. Chem. Theo. Comput.*, 2022, **18**, 3497–3511.

26 A. Krzemińska, M. Biczysko, K. Pernal and M. Hapka, *J. Phys. Chem. A*, 2024, **128**, 8816–8824.

27 G. Bistoni, *WIREs Comput. Mol. Sci.*, 2020, **10**, e1442.

28 T. Yanai, D. P. Tew and N. C. Handy, *Chem. Phys. Lett.*, 2004, **393**, 51–57.

29 A. D. Becke, *J. Chem. Phys.*, 1993, **98**, 5648–5652.

30 C. Lee, W. Yang and R. G. Parr, *Phys. Rev. B: Condens. Matter Mater. Phys.*, 1988, **37**, 785–789.

31 F. Weigend, *Phys. Chem. Chem. Phys.*, 2006, **8**, 1057–1065.

32 S. Grimme, S. Ehrlich and L. Goerigk, *J. Comput. Chem.*, 2011, **32**, 1456–1465.

33 A. Altun, R. Izsák and G. Bistoni, *Int. J. Quantum Chem.*, 2021, **121**, e26339.

34 A. Altun, F. Neese and G. Bistoni, *Beilstein J. Org. Chem.*, 2018, **14**, 919–929.

35 A. Altun, F. Neese and G. Bistoni, *J. Chem. Theory Comput.*, 2019, **15**, 215–228.

36 W. B. Schneider, G. Bistoni, M. Sparta, M. Saitow, C. Riplinger, A. A. Auer and F. Neese, *J. Chem. Theory Comput.*, 2016, **12**, 4778–4792.

37 C. Riplinger, B. Sandhoefer, A. Hansen and F. Neese, *J. Chem. Phys.*, 2013, **139**, 134101.

38 Y. Guo, C. Riplinger, U. Becker, D. G. Liakos, Y. Minenkov, L. Cavallo and F. Neese, *J. Chem. Phys.*, 2018, **148**, 011101.

39 A. Hellweg, C. Hättig, S. Höfener and W. Klopper, *Theor. Chem. Acc.*, 2007, **117**, 587–597.

40 F. Neese, F. Wennmohs, U. Becker and C. Riplinger, *J. Chem. Phys.*, 2020, **152**, 224108.

41 F. Neese, *Wiley Interdiscip. Rev.: Comput. Mol. Sci.*, 2022, **12**, e1606.

42 M. D. Hanwell, D. E. Curtis, D. C. Lonie, T. Vandermeersch, E. Zurek and G. R. Hutchison, *J. Cheminf.*, 2012, **4**, 17.

43 A. Wuttke and R. A. Mata, *J. Comput. Chem.*, 2016, **38**, 15–23.

44 E. C. Meng, T. D. Goddard, E. F. Pettersen, G. S. Couch, Z. J. Pearson, J. H. Morris and T. E. Ferrin, *Protein Sci.*, 2023, **32**, e4792.

45 N. C. Baird, *J. Am. Chem. Soc.*, 1972, **94**, 4941–4948.

46 M. Rosenberg, C. Dahlstrand, K. KilsÅ and H. Ottosson, *Chem. Rev.*, 2014, **114**, 5379–5425.

47 J. Yan, T. Slanina, J. Bergman and H. Ottosson, *Chem. – Eur. J.*, 2023, **29**, e202203748.

48 M. H. Palmer, M. Coreno, M. de Simone, C. Grazioli, N. C. Jones, S. V. Hoffmann, R. A. Aitken and D. K. Sonecha, *J. Chem. Phys.*, 2023, **158**, 014304.

49 S. G. Chiodo and N. Russo, *Chem. Phys. Lett.*, 2010, **490**, 90–96.

50 European Organization For Nuclear Research and OpenAIRE, Zenodo, 2013, **https://www.zenodo.org/**.

51 F. Dietrich, *Data for Influence of Substitution Patterns on Isomer Preference in Chromone–Methanol Clusters*, 2025, DOI: **10.5281/zenodo.14750557**.

